

Visual stratigraphy of the North Greenland Ice Core Project (NorthGRIP) ice core during the last glacial period

Anders Svensson,¹ Søren Wedel Nielsen,¹ Sepp Kipfstuhl,² Sigfus J. Johnsen,¹ Jørgen Peder Steffensen,¹ Matthias Bigler,³ Urs Ruth,² and Regine Röthlisberger³

Received 16 June 2004; revised 5 October 2004; accepted 24 November 2004; published 21 January 2005.

[1] A continuous high-resolution record of digital images has been obtained from the North Greenland Ice Core Project (NorthGRIP) ice core (75.1°N, 42.3°W) in the depth interval from 1330 m to the bedrock at 3085 m. The ice core stratigraphy is clearly visible throughout the glacial period with the most frequent and brightest visible layers appearing during the coldest events. Down to a depth of 2600 m the horizontal layering is very regular; below this depth, small irregularities in the layering start to appear, and below 2800 m the visual stratigraphy becomes more uncertain, perhaps because of penetration into climatically warmer ice. Comparison of the visual stratigraphy with high-resolution continuous records of chemical impurities and dust reveals a high degree of correlation, which indicates that the visible layers are caused by these impurities. A new approach is used to automatically determine annual layer thicknesses from the visual stratigraphy record by carrying out a frequency analysis of the most prominent visible layers in the profile. The result gives strong support for the NorthGRIP timescale model.

Citation: Svensson, A., S. W. Nielsen, S. Kipfstuhl, S. J. Johnsen, J. P. Steffensen, M. Bigler, U. Ruth, and R. Röthlisberger (2005), Visual stratigraphy of the North Greenland Ice Core Project (NorthGRIP) ice core during the last glacial period, *J. Geophys. Res.*, *110*, D02108, doi:10.1029/2004JD005134.

1. Introduction

[2] The visual stratigraphy (VS) is probably the most basic information one can obtain from an ice core. All Greenland ice cores reaching into glacial ice have been reported to reveal bands of cloudy and clear ice [e.g., Meese *et al.*, 1997; Shimohara *et al.*, 2003], but in existing studies VS profiles are documented as drawings or as photographs, which have limited resolution and dynamical range. One of the most extensive investigations of ice core VS is that of the GISP2 ice core from central Greenland [Meese *et al.*, 1997] from which the dating was partially based [Alley *et al.*, 1997b]. Recently, the development of the digital scanners, computers, and large storage media, has opened up new possibilities for obtaining, storing, and treating high-resolution VS profiles.

[3] The North Greenland Ice Core Project (NorthGRIP) retrieved an ice core in northern Greenland during the summers of 1996–2003 [Dahl-Jensen *et al.*, 2002; North Greenland Ice-Core Project (NorthGRIP) Members, 2004]. The ice core is 3085 m long and covers the Holocene, the

entire last glacial period, and part of the previous interglacial period, the Eemian, back to approximately 123 kyr BP. In 2003, when drilling was terminated, it was discovered that basal melting occurs at the site. Because of the melt, the thinning of the deep NorthGRIP ice is relatively small compared to other Greenland locations where the ice is frozen to bedrock, and therefore the annual layer thickness in the deep NorthGRIP ice is high, of the order of 1 cm. The high resolution, combined with a flat subglacial bed at NorthGRIP, offers the unique possibility to improve the existing timescales based on annual layer counting of the glacial period and possibly the glacial inception after the last interglacial period.

[4] In this paper we present the VS profile (also known as the line scan profile) of the NorthGRIP ice core, which has been obtained with an automated line scan instrument and stored as digital images. We discuss the relation between VS and impurities in the ice, and the potential for using VS to date glacial ice.

2. Methods

[5] The NorthGRIP VS profile continuously covers the depth interval 1330–3085 m, which corresponds to the time interval 9–123 kyr BP. For the depth interval 1330–2930 m, the profile was obtained in the field during the summer of 2000. The ice from 1330–1750 m depth had been drilled during the season of 1999 and had been stored at NorthGRIP at temperatures below -20°C for one year prior to

¹Department of Geophysics, University of Copenhagen, Copenhagen, Denmark.

²Department of Geophysics/Glaciology, Alfred Wegener Institute for Polar and Marine Research, Bremerhaven, Germany.

³Climate and Environmental Physics, Physics Institute, University of Bern, Bern, Switzerland.

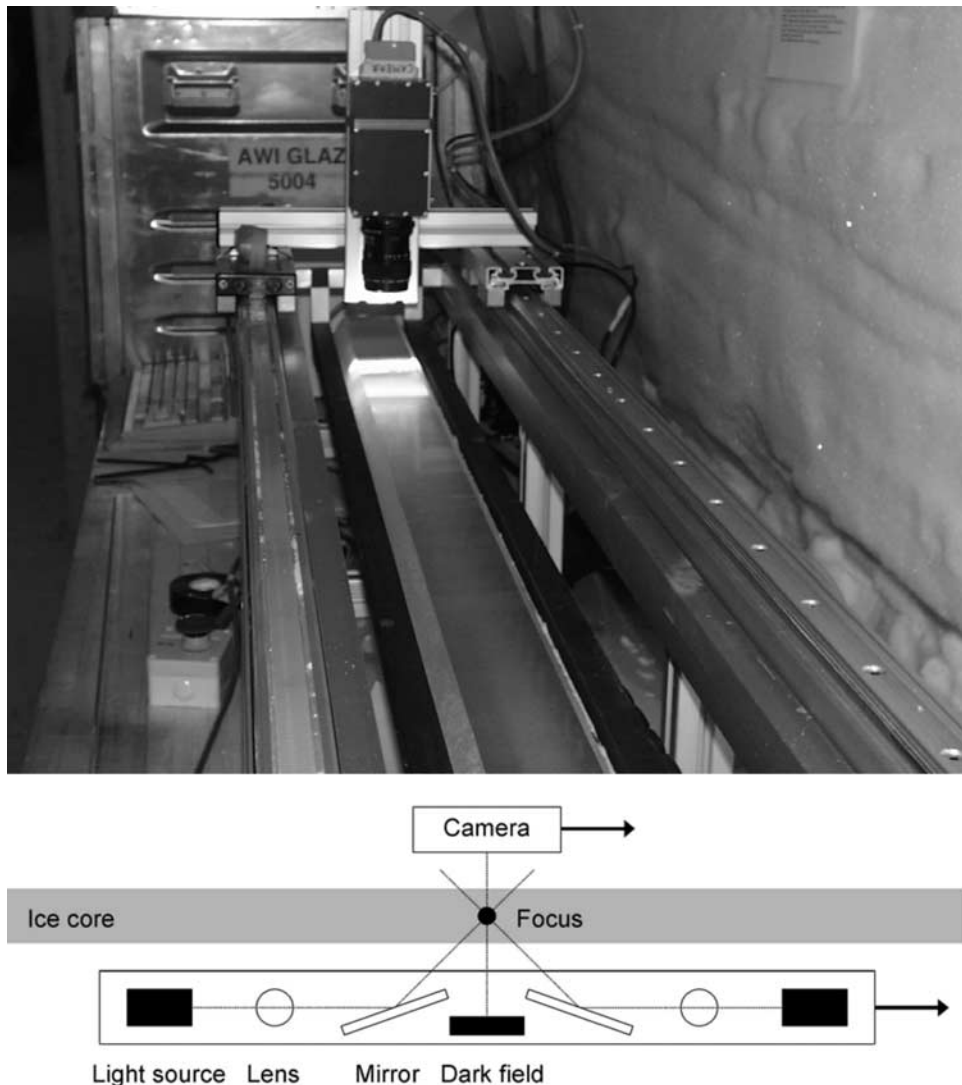


Figure 1. (top) Line scan instrument in operation. A camera is moving along the upper side of a 1.65 m long ice core section, while an indirect light source is moving below the ice. (bottom) Schematic drawing demonstrating the principle of the line scan instrument. The light from the source enters the ice at an angle of 45° , so that the camera detects only light that is scattered in the ice. Transparent ice thus appears black in the record.

measurement, while the deeper ice was measured within weeks after recovery. The depth intervals 2930–3001 m and 3001–3085 m were measured at the Alfred Wegener Institute for Polar and Marine Research (AWI), Bremerhaven, Germany, within a few months after recovery in 2001 and 2003, respectively.

[6] The measurement was carried out on a line scan instrument designed at AWI and later modified at the Niels Bohr Institute, Copenhagen. 1.65 m long, 3 cm thick, and 8–9 cm wide slabs of ice core were carefully microtomed on both sides and imaged at a resolution of 118 pixels per centimeter (Figure 1). The measuring principle is comparable to that of dark field microscopy: An indirect light source and a camera are mounted on two trolleys located below and above the ice core section. The trolleys move synchronously along the ice and the camera records the light that is

scattered in the ice. In the obtained images, transparent ice appears black while any visible obstacles in the ice, such as visible layers or bubbles, appear white.

[7] The camera originally measured light intensities in 8-bit resolution, but because of a failure of the most significant bit of the camera, the effective dynamical range of pixel intensities in the obtained images is 7 bit. This failure caused a saturation problem for bright cloudy bands in the profile. However, for most of the measurements, saturation was avoided by adjusting the light source diaphragm aperture according to the brightness of visible layers in the ice, and thus the profile is not seriously disturbed by the problem.

[8] During the 2000 NorthGRIP field season several other high-resolution measurements were obtained from the NorthGRIP ice core. The mass concentration of water-

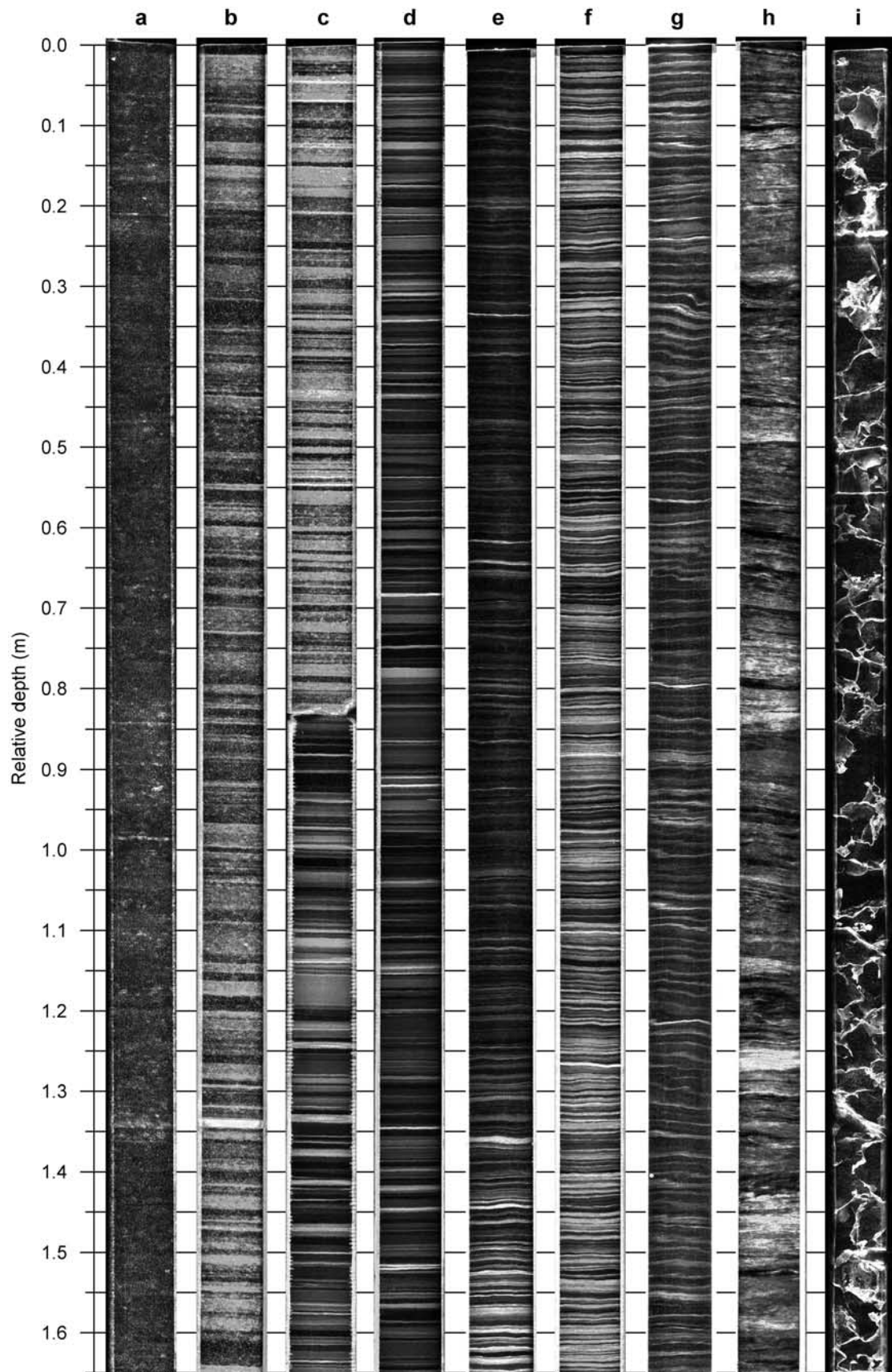


Figure 2

soluble calcium Ca^{++} , sodium Na^+ , ammonium NH_4^+ , sulphate SO_4^{--} , nitrate NO_3^- , the electrolytical conductivity of the melt water, and the amount of insoluble dust were measured by continuous flow analysis (CFA) on the ice core section that was previously used for the VS measurement [Bigler, 2004; Röthlisberger *et al.*, 2000; Ruth *et al.*, 2003].

3. Results

[9] The obtained VS profile is generally of very high quality and provides a detailed visual documentation of the entire glacial part of the NorthGRIP ice core, in addition to 160 m of Preboreal ice (1330–1490 m depth) and 100 m of Eemian ice (2985–3085 m depth) (Figure 2).

[10] Compared to most of the glacial ice, the Holocene ice is characterized by being rather transparent (Figure 2a). In the Holocene ice, bright layers or regions occur occasionally but not at regular intervals. At high resolution, millimeter-sized bright patches in the images can be identified as ice crystal interfaces that have become visible because of relaxation of the ice. Small submillimeter-sized spots are air bubbles, whereas clear (dark) layers of ice have been identified as possible melt layers or ice where bubbles have converted into clathrate hydrates (Figure 3a) [Kipfstuhl *et al.*, 2001].

[11] Throughout the glacial period, the ice core stratigraphy is clearly visible. During the coldest climatic events the intensity and the frequency of visible layers or cloudy bands are highest (Figures 2b–2d). During milder interstadials the layering is also clearly visible after contrast enhancement of the images, even when the stratigraphy of the core is barely visible to the naked eye. An example of an abrupt climatic transition during the glacial period is given in Figure 2e, which shows the transition into the mild glacial interstadial 19 as a sharp drop in intensity of the VS over some 10 cm of ice. The glacial profile is very detailed and reveals very sharp transitions in the occurrence of visible layers, which show a large variability in intensity and thickness even over short depth intervals (Figure 3c).

[12] A very distinct transition between ice drilled during the 1999 season and ice recovered in the 2000 season is found at 1751.5 m depth (Figure 2c). The ice that has been stored for one year at NorthGRIP shows much more pronounced cloudy bands than the freshly drilled ice. Also the density of “white patches” and bubbles are much higher in the stored ice. This clearly demonstrates that the internal structure of the ice core relaxes after recovery, even when

the ice is stored under optimal cold conditions. Similar observations have been made for the GISP2 ice core [Meese *et al.*, 1997; Ram *et al.*, 2000].

[13] Down to a depth of about 2600 m the horizontal layering of the ice is very regular (Figure 2f). Below this depth smaller disturbances in the layering such as micro folds start to appear (Figures 2g and 3d). Such disturbances were also observed in the deep parts of the GISP2 and GRIP ice cores [Alley *et al.*, 1997a; Dahl-Jensen *et al.*, 1997] where they were ascribed to the rotation of assemblies of ice crystals (shear faults or stripes) in the strongly anisotropic ice. Fabric measurements of the deep NorthGRIP ice suggest that the flow regime of the ice changes around 2500 m depth from a confined compression to a simple shear deformation characterized by a strong single maximum fabric [Wang *et al.*, 2002]. Below 2630 m depth a weakening in the strength of the single maximum fabric indicates that other processes than simple shear have become active in the deformation of the ice.

[14] Below 2800 m the visual stratigraphy becomes more uncertain with more diffuse and inclined layering, and in some depth intervals it is impossible to distinguish individual layers (Figure 2h). Although the stratigraphy may appear disturbed at this depth, it should be kept in mind that the line scan measurement is averaging over a 3 cm thick slab of ice, so that even a small inclination of well separated layers in the ice may result in a smearing out of the stratigraphy in the line scan images.

[15] An important factor in the deep NorthGRIP ice is the warm temperature, which increases with depth to the pressure melting point of -2.4°C at the base (3085 m depth). At such warm temperatures, the crystal growth rate is very high and annealing recrystallization becomes important. It is likely that a very active ice crystal boundary migration has influenced the distribution of soluble impurities in the ice and thereby disturbed the ice core stratigraphy [Barnes *et al.*, 2003]. The ice crystals in the deepest ice are large, of the order of 1–10 cm diameter, and in the lowest 100 m of the ice core, ice crystal boundaries are visible in the line scan images (Figure 2i). Centimeter-sized ice crystals have also been observed in deepest part of the GRIP and GISP2 ice cores [Gow *et al.*, 1997; Thorsteinsson *et al.*, 1997], but because of the warmer temperatures the NorthGRIP crystals are even larger.

[16] Clearly visible volcanic ash layers in the ice can be identified as very bright layers in the line scan profile, which, however, appear quite similar to intense cloudy bands (Figures 2b and 3b). Many of the known volcanic

Figure 2. Examples of line scan images from various depths. Each ice section is 1.65 m long, 3 cm thick, and 8–9 cm wide. In order to visualize the stratigraphy the contrast of the images is enhanced. The bright lines on the sides of the ice are due to light reflected from the curved outer surface of the ice core. (a) Holocene ice, 1354.65–1356.30 m depth. White patches are most likely ice crystal interfaces within the ice. (b) Ice from the Younger Dryas, 1504.80–1506.45 m depth. The bright layer at 1.33 m relative depth is the volcanic “Vedde” ash layer (see also Figure 3b). (c) Transition from ice drilled during the 1999 field season and that from the 2000 season in cold glacial ice, 1750.65–1752.30 m depth. (d) Ice from around Last Glacial Maximum, 1836.45–1838.10 m depth. (e) Ice from the sharp climatic transition into the mild glacial interstadial 19 (IS19) at 2534.40–2536.05 m depth. The transition is clearly seen in the lower half meter of the core. (f) Ice from the cold period preceding IS19 at 2537.70–2539.35 m depth. The horizontal layering is still very regular at this depth. (g) Microfolding starts to appear below 2600 m. Here is an example from 2651.55–2653.20 m depth. (h) 2899.05–2900.70 m depth. The overall horizontal layering is still obvious, but individual cloudy bands are not distinguishable. (i) 3017.30–3018.95 m depth. Visible grain boundaries of large crystals.

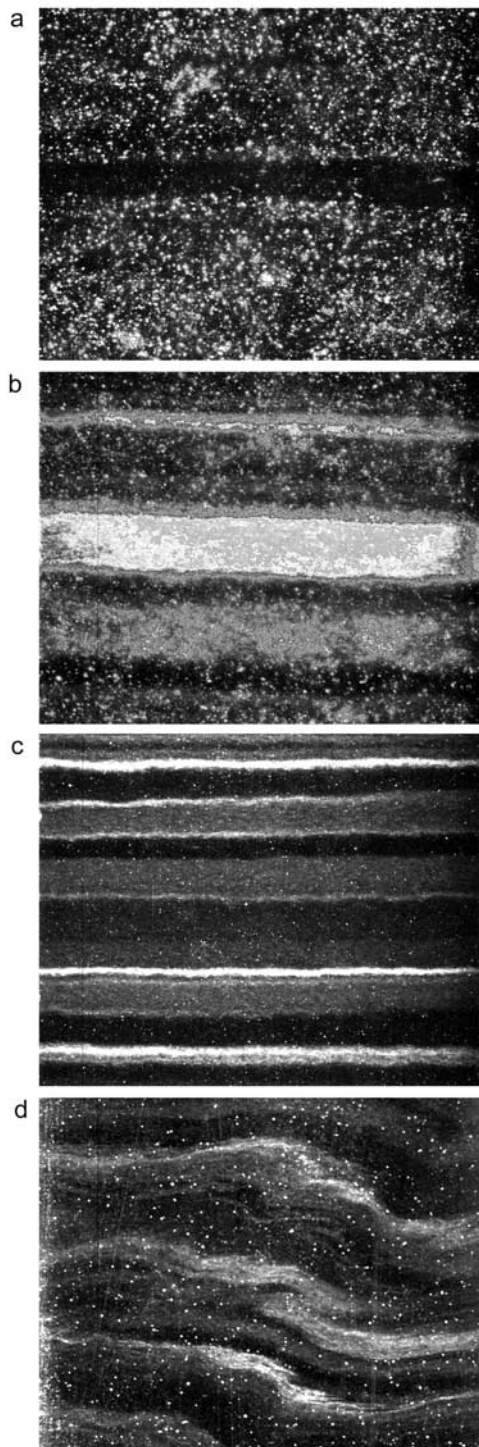


Figure 3. Close-up examples of line scan images. The sections shown are 6 cm high and 7.5 cm wide, and the contrast of the images has been enhanced. (a) 1412.1 m depth, Holocene ice with visible air bubbles. The band of clear (dark) ice indicates a possible melt layer or ice where the air bubbles are converted into clathrate hydrates. (b) 1506.1 m depth, the visible “Vedde” ash layer in Younger Dryas (also shown in Figure 2b). (c) 1836.9 m depth. There is detailed layering around Last Glacial Maximum. (d) Example of microfolding at 2675.0 m depth. At greater depths the layering is again more regular.

horizons in the glacial profile, which contain low concentrations of volcanic tephra (A. K. Mortensen et al., Ash layers from the last glacial termination in the NGRIP ice core, submitted to *Journal of Quaternary Science*, 2004), are barely or not at all distinguishable in the VS profile.

[17] Figure 4 shows the intensity or grey value profile obtained from averaging the intensity of the line scan images over 165 cm sections. The profile is corrected for intensity changes of the light source of the instrument, and the section corresponding to ice drilled in 1999 (above 1751.5 m depth) has been rescaled to compensate for the “ageing effect” of more pronounced cloudy bands in that ice. The intensity of the ice drilled in 2001 and 2003 (below 2930 m depth) has also been rescaled because of its higher intensity level due to relaxation and the appearance of crystal boundaries in the ice. Furthermore, physical breaks and fractures in the ice core, which typically can be identified as bright areas in the VS profile, have not been removed and introduce some noise in the profile.

[18] The overall characteristics of the intensity profile clearly resemble the well-known chemical concentration profiles of Greenland glacial ice cores, and except for an elevated background level the VS intensity profile is very similar to that of the dust concentration (Figure 4). Cold climatic periods have on average a high density of visible layers and thus “bright intensity,” whereas milder periods have more transparent ice. The strongest intensities are found in the two peaks around the last glacial maximum (approximately 1800 m depth), which are characteristic for the concentration profiles of Ca^{++} and insoluble mineral dust, but not for the other chemical profiles.

4. Visual Stratigraphy and Impurities

[19] The occurrence of cloudy bands in glacial ice with high concentrations of dust and other impurities has long been recognized [e.g., *Ram and Koenig*, 1997], but it remains a question what those visible layers in the ice actually represent and how they relate to the various impurities in the ice. With the new NorthGRIP high-resolution VS and CFA records we now have the possibility to investigate these layers in more detail.

[20] A comparison between the VS and CFA profiles for 1.65 m of ice from one of the coldest periods during the last glacial is given in Figure 5. This is around 1908 m depth where the impurity concentration of the ice is high, and the annual layer thickness is of the order of 1.5 cm. The line scan image and the corresponding light intensity curve are shown along with the mass concentration of dust, Ca^{++} , Na^+ , NH_4^+ , SO_4^{--} , NO_3^- , and the electrolytical conductivity of the melted ice. The raw VS intensity profile has much higher resolution than the CFA profiles. When the VS intensity profile is smoothed with Gaussian filters representative for the various chemical components, the VS data actually reproduce many of the features of the CFA profiles. For example, it is remarkable how well the VS intensity profile smoothed with a 1.3 cm broad Gaussian (2σ) resembles the electrolytical conductivity profile. Essentially, every peak in the conductivity profile appears in the smoothed line scan profile, whereas the relative amplitudes do not always reproduce. When smoothed with a broader Gaussian the VS profile also mimics the Ca^{++} and dust

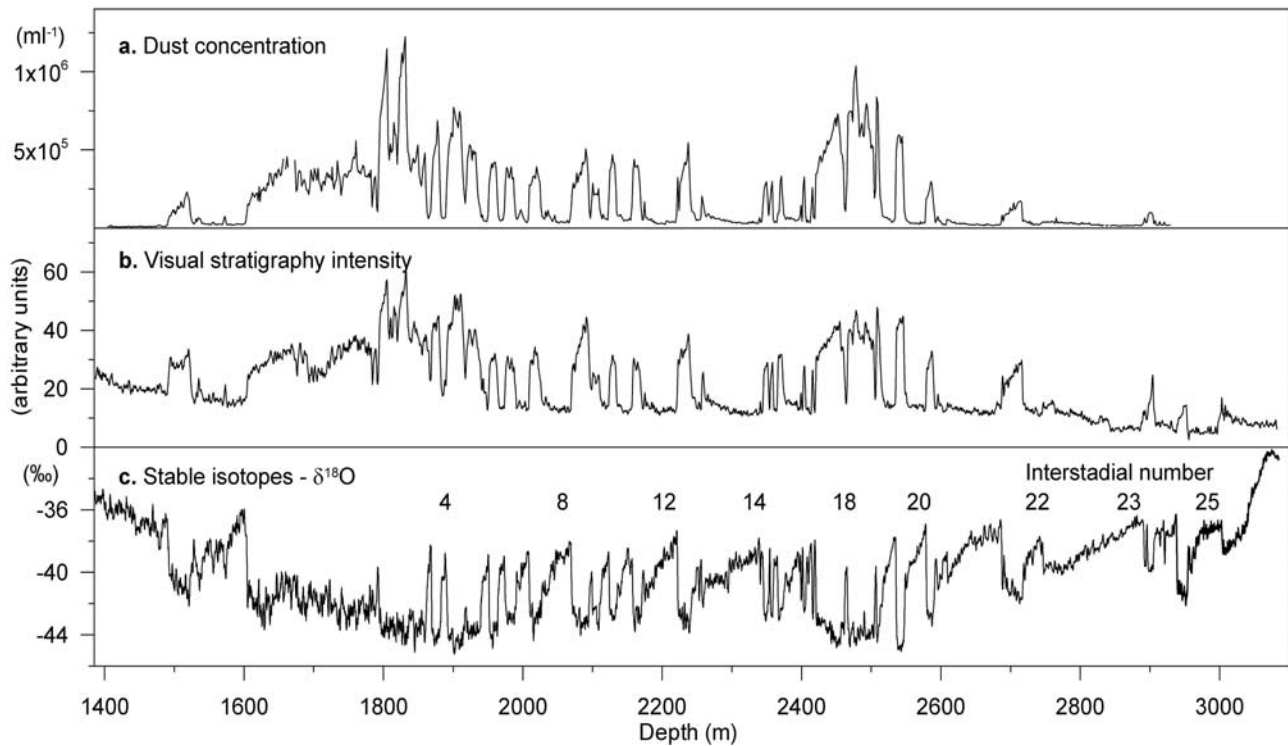


Figure 4. (a) NorthGRIP insoluble dust profile shown as the number concentration of particles larger than $1\ \mu\text{m}$ [Ruth *et al.*, 2003]. (b) Line scan intensity (grey value) profile. (c) The $\delta^{18}\text{O}$ profile [North Greenland Ice-Core Project (NorthGRIP) Members, 2004]. All profiles are 165 cm averages. The intensity profile has been scaled to be continuous across the transition at 1751 m depth, which separates ice that was drilled in the field season of 1999 and 2000. Intensity values from above 1751 m depth are multiplied by a factor of 2/3 to compensate for the more pronounced cloudy bands in the stored ice. The intensity of the ice drilled and measured in 2001 and 2003 (below 2930 m depth) is strongly influenced by the visible grain boundaries, and it has been rescaled by a factor of 1/4. The line scan intensity is extracted from the raw images without removal of breaks or other features.

concentration profiles very well. The smoothed intensity curve also resembles the Na^+ , NH_4^+ , SO_4^{2-} , and NO_3^- profiles to some degree, but the correspondence is less obvious. Several peaks in those profiles are either absent or less pronounced than in the VS profile.

[21] Inspections of the CFA and VS profiles at other depths show that the striking similarity between the VS intensity curve on the one hand and the electrolytical conductivity, dust, and Ca^{++} on the other hand is characteristic for all of the glacial ice, although it is most pronounced for the cold glacial periods. The strong correlation between VS and the dust/ Ca^{++} concentration of the ice strongly suggests that the cloudy bands are caused by these impurities. This result is in good accordance with observations from the glacial part of the GISP2 ice core [Alley *et al.*, 1997b], where continuous measurements of 90° laser-light scattering on the solid ice correlate well with the dust concentration of the melted ice [Ram and Koenig, 1997].

[22] It has been suggested that cloudy bands appear because of microbubbles that form around the impurities [Dahl-Jensen *et al.*, 1997; Shimohara *et al.*, 2003]. However, preliminary experiments performed by S. Kipfstuhl suggest that it is actually particulate matter in the ice that makes the cloudy bands visible: When cloudy band ice is melted with alcohol and observed under a microscope, the

inclusions are hit by the melt front without the appearance of small “explosions” that characterize melting of ice containing high-pressure bubbles. If this is true, it is unlikely that other impurities than insoluble dust contribute significantly to the cloudy bands, because other impurities are too small to be visible.

[23] We suggest that the VS profile represents the depositional history at NorthGRIP, i.e., that each cloudy or clear layer in the ice represents a depositional event, and that the intensity of each layer is related to the impurity content of that layer. By a depositional event we mean either precipitation or the formation of sastrugis by wind-driven redistribution of surface snow. The very thin and bright cloudy bands occurring in the cold glacial periods (e.g., Figure 3c) could possibly be associated with enhanced scavenging early in a snowfall, or with periods of low precipitation and dry deposition. In the deeper ice where thinning becomes more important it is no longer possible to distinguish individual depositional events.

[24] The VS images may help identifying where in the ice crystal structure the visible impurities are located. For the late glacial period, the homogeneity in intensity of individual cloudy bands (Figure 3c) suggests that the impurities are evenly distributed within the ice lattice, i.e., that most impurities are situated within the bulk of the ice crystals.

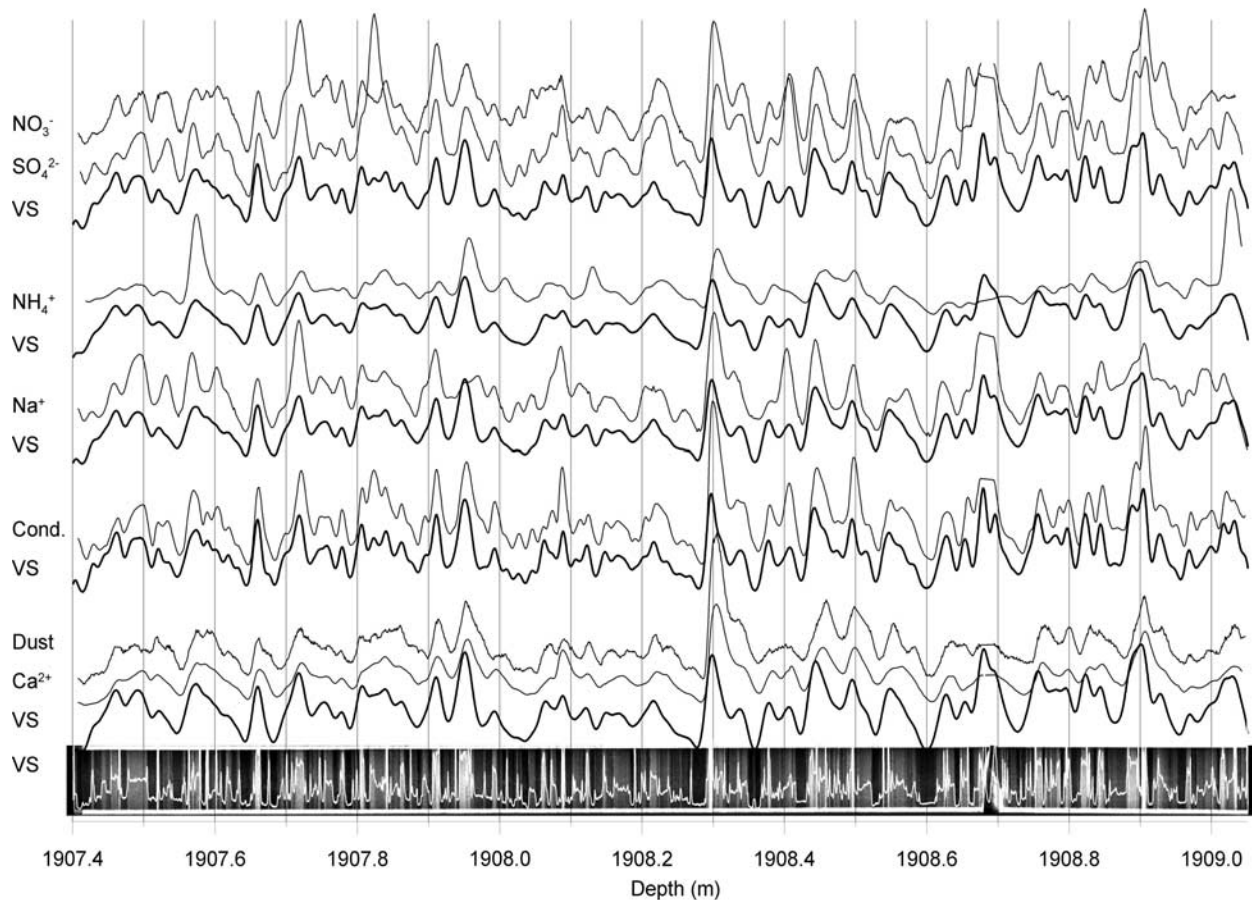


Figure 5. Comparison between visual stratigraphy (VS) and impurity concentrations of the ice at 1907.40–1909.05 m depth. All units are arbitrary, and the linear scales have been adjusted to facilitate comparison. Just above 1908.70 m is a break in the core, which has not been removed in the line scan profile. At the bottom is shown the line scan image superimposed by the corresponding intensity profile. The VS intensity curve has been smoothed with Gaussian filters of different widths (five thick curves) in order to make the best comparison to the CFA profiles (seven thin curves). The CFA profiles shown are (from top to bottom) NO_3^- , SO_4^{2-} , NH_4^+ , Na^+ , electrolytical conductivity, dust, and Ca^{++} . The 2σ widths of the Gaussians used for smoothing the intensity profiles are (from top to bottom) 1.5, 2.1, 1.7, 1.3, and 1.9 cm.

This finding agrees with that of *Barnes et al.* [2002], who determined an even distribution of dust particles within one late glacial GRIP ice core section. At greater depths, the less regularity of the cloudy bands (Figure 3d) indicates that the impurities may have been displaced, perhaps toward the crystal boundaries. In the deepest ice, where crystal boundaries are clearly visible in the VS record, it is possible that a large fraction of the impurities has been moved to the crystal boundaries by ice rheology. However, the conditions in the deepest ice are not directly comparable to those of the glacial ice because of the high temperatures near the bottom and because the climatically warm ice has very low impurity content.

[25] For the preboreal ice, where cloudy bands are rare, there is a much weaker correspondence between the VS intensity and the various CFA components compared to glacial ice, although strong NH_4^+ and acidity peaks are sometimes visible in the stratigraphy. One reason for this

is probably the presence of air bubbles in the preboreal ice, which contribute substantially to the VS intensity profile. The relaxation effect, caused by the storing of the ice, which strongly affects the low-intensity VS profile, also tends to obscure a possible correspondence between VS and impurities in the preboreal ice.

5. Ice Core Dating

[26] The high temporal resolution of the NorthGRIP ice core during the glacial period makes the core an obvious candidate for obtaining a high-precision counted timescale of that period. Because the line scan measurements are made directly on the ice, the profile has a high depth resolution and a well-determined depth control. Therefore the line scan profile with its clearly identifiable layers, is tempting to apply as a tool for an absolute dating of the glacial period, especially in the deeper part of the ice core,

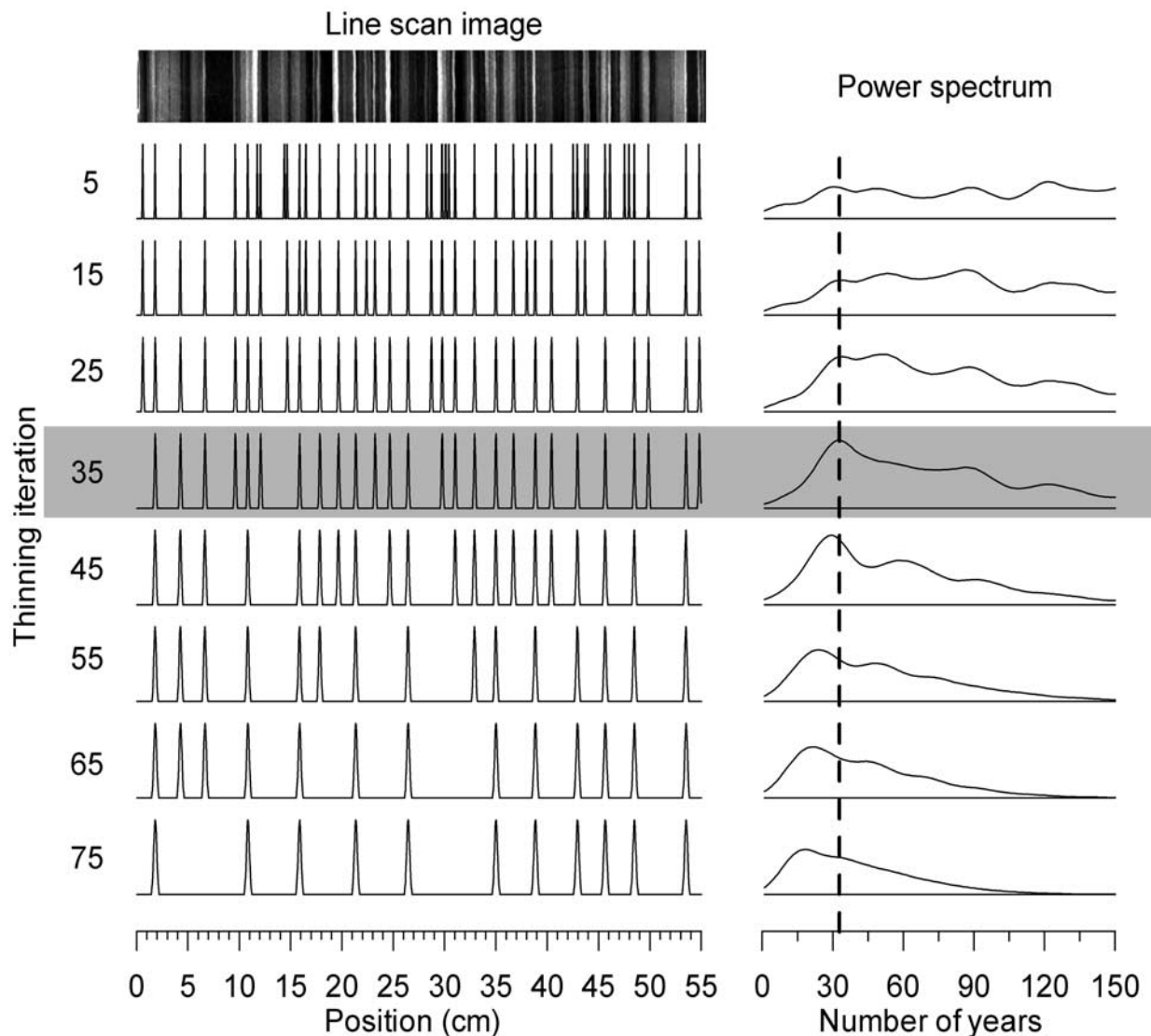


Figure 6. Snapshot example (1879.35–1879.90 m depth) of the method applied in this study to obtain the annual layer thicknesses from the line scan profile. First, the line scan image is “digitized” into an array of lines at the positions of the most prominent cloudy layers (top left corner). This array is then iteratively thinned by removal of closest neighbors (left-hand side), and the corresponding power spectra are obtained (right-hand side). The power spectra are normalized and weighted by the number of remaining lines in the thinned arrays. The annual layer thickness of the ice is identified from the maximum power of the obtained power spectra, which occurs at iteration 35 (grey horizontal bar). The frequency corresponding to strongest power occurs at 34 annual layers (vertical dashed line) or, equivalently, an annual layer thickness of 1.6 cm.

where no other existing record has the resolution necessary to resolve annual layers.

[27] An important question in this context is how well the glacial VS profile actually provides an annual signal [Alley *et al.*, 1997b; Meese *et al.*, 1997]. As discussed previously, the cloudy bands are likely to be related to depositional events with high dust content. The flux of dust to the ice is known to show a seasonal variation [Ram and Koenig, 1997], but because some years may experience more depositional events than others, some annual layers will appear as multiple visible layers in the VS profile, while others may only be weakly represented in the stratigraphy. Inspection of the VS profile, at depths where the annual

layers can be identified from the CFA profiles, shows that “multiple-layer” years appear frequently. Another difficulty is caused by the great variability in intensity of the visible layers, which complicates the counting. Depending on the contrast enhancement of the images and on the selection criteria used for identifying the layers, one can end up counting a wide range of layers within the same ice core section, e.g., as the contrast of an image is increased, more and more layers tend to appear. For those reasons, accurate dating from direct counting of the VS profile alone generally has proven difficult.

[28] One way to overcome the multiple-layer problem for annual layer counting is to smooth the intensity profile such

as proposed by *Shimohara et al.* [2003] in a case study of 10 sections of GRIP and NorthGRIP glacial ice. Although this approach is promising, the smoothing method assumes preknowledge of the mean annual layer thickness from modeling, which may not always be justified. Furthermore, the number of annual layers that is identified within a section of ice is likely to vary with the width of the filter applied for smoothing the profile.

[29] A different approach to obtain a chronology from the VS record consists in applying a frequency analysis to sections of the VS intensity profile. This approach has the advantage of being less sensitive to “weak layer” or “multiple-layer” years, because it determines an overall frequency for the entire section that is less dependent on the appearance of individual years. On the other hand, a successful outcome of such a method requires a certain regularity in the annual layer thicknesses within each considered section. Experience shows that generally an annual peak appears in the power spectrum obtained from a section of the VS intensity profile, but often the peak is obscured, because of the pronounced variability in intensity and thickness of the individual cloudy bands.

[30] In this work, we undertake a two-step method for automatic determination of the annual layer thicknesses of the glacial ice from the VS intensity profile. The line scan images are treated in 55 cm sections, and the principle of the method is demonstrated for one such section in Figure 6.

[31] In a first step, the line scan profile is “digitized” by identifying the most prominent cloudy bands in the section: The intensity distribution of the line scan image is equalized in order to give emphasis to weaker cloudy bands, and the depths corresponding to the onset of the cloudy bands are determined from the strongest positive intensity gradients in the intensity-calibrated image. This results in an array of depths at the onsets of the most prominent visible layers. By undertaking this digitalization we overcome to some degree the problem of variable intensity and duration of individual cloudy bands, because each band now is given the same “weight.” The number of cloudy bands identified in each 55 cm section depends on the annual layer thickness. Up to 65 cloudy bands are identified when annual layers are thin, but in milder periods as few as 10 layers may be found. At this point, a fraction of the annual layers may be represented by multiple cloudy bands in the array.

[32] In the second step, the array of cloudy bands is iteratively thinned by removal of closest neighbors. For each iteration, an increasingly large minimum distance between each two cloudy bands is required, and if two cloudy bands are closer than this minimum distance, one of them is removed at random. The idea of the thinning procedure is to reduce multiple-layer years to single-layer years, and the random removal approach is applied because we have no way of judging which of the cloudy bands best represents the position of the mean annual layer. For each iteration, the thinned array is smoothed with a Gaussian filter and subsequently a power spectrum is obtained. The power spectrum is normalized to have an integral value of one, and weighted by the number of cloudy bands in the thinned array. This weighing procedure is undertaken in order to enable a comparison of the power spectra obtained for each iteration step. Finally, the annual layer thickness is determined as corresponding to the frequency that shows

the maximum power in the obtained power spectra. The iteration at which the annual layer thickness is determined may have up to 50% of the identified layers removed by thinning, but most often less layers are removed.

[33] Because of the random removal procedure utilized to thin the array, the progressive thinning of an array can evolve in manifold ways. Experience shows that generally the majority of those thinning schemes lead to practically the same annual layer thickness, but that some schemes may diverge and result in outliers. In order to avoid these outliers 20 arrays are thinned in parallel through each iteration step and the power spectra of those are added before the annual layer thickness is identified.

[34] It frequently appears that annual layers are so weakly represented by cloudy bands that the automatic method cannot identify them. However, because our method is based on a frequency analysis, it is not so critical if a few annual layers are missing as long as the bulk of cloudy bands are identified. For a number of ice core sections a large fraction of annual layers could not be identified, typically when the section contains a physical break that dominates the high intensities of the image. In those cases the intensity calibration of the image is made manually.

[35] The above described method makes use of a number of adjustable parameters, e.g., the threshold criteria for the gradient in selection of “most prominent” cloudy layers, the width of the Gaussian filter used for smoothing of the array prior to obtaining the power spectrum, and the weighing factor of the normalized power spectra. The result of the method depends on the choice of those parameters and they therefore need some calibration. For this study, the parameters have been tuned to obtain the best possible fit with the modeled annual layer thicknesses obtained by the $\delta^{18}\text{O}$ -based model “ss09sea” [*Johnsen et al.*, 2001; *North Greenland Ice-Core Project (NorthGRIP) Members*, 2004].

[36] The method is applied for depths greater than 1800 m only. Above 1750 m depth the VS profile has the problem of relaxation, caused by the storing of the ice, which introduces noise into the VS intensity profile and dampens the annual signal (causing our approach to malfunction). The result of the analysis is shown in Figure 7. The obtained annual layer thickness profile is seen to vary consistently in accordance with climate showing thin annual layers during cold periods and thicker annual layers during periods with milder climate. Furthermore, the annual layer thinning apparently decreases in the deeper part of the ice, so that layer thicknesses of 1–1.5 cm is maintained in the depth interval 2600–2700 m, where the ice is more than 80 kyr old. Below 2720 m depth the layering of the core becomes too irregular for the method to function, and the determined annual layers are unrealistic.

[37] Generally, the obtained annual layer thicknesses are seen to be in good agreement with the NorthGRIP “ss09sea” timescale model. Of course, one can argue that since the ss09sea model was used for calibration of our method, a good correspondence between the two is anticipated. However, it should be stressed that with the exception of a number of outliers, the entire VS profile has been treated in exactly the same way, e.g., the same parameter setting has been applied for the analysis at all depths. With only a limited number of parameters to vary there is a limit

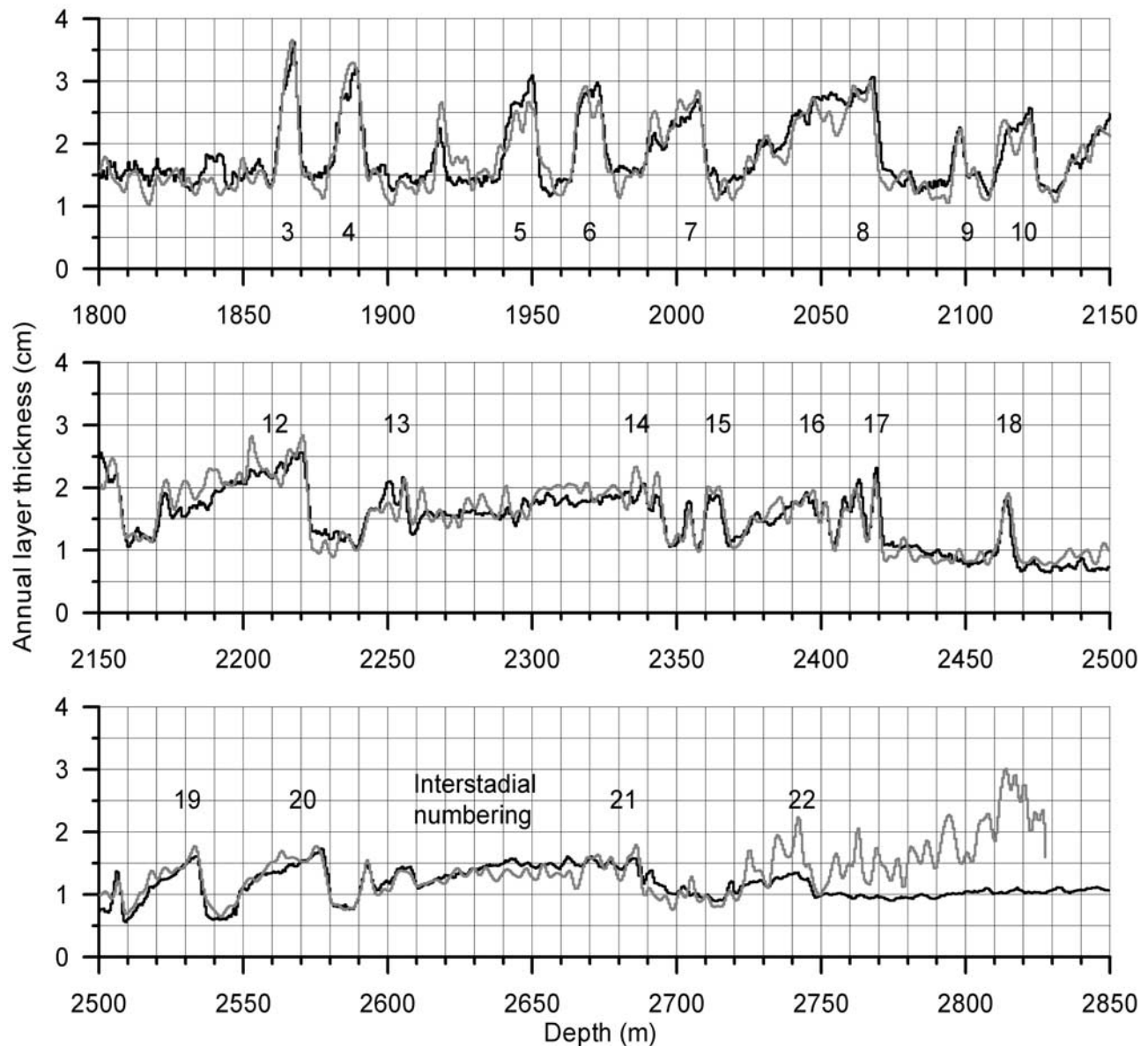


Figure 7. Annual layer thickness profile obtained in this study from the line scan images (grey curve) compared to that of the $\delta^{18}\text{O}$ -based “ss09sea” model (black curve), which has been transferred from the GRIP ice core by reference horizons. The line scan curve has been smoothed in order to facilitate comparison.

to how much the resulting profile can be manipulated. Basically, a different choice of parameters can change the appearance of the entire profile, whereas it cannot introduce or remove localized features in the profile, such as the enhanced annual layer thicknesses occurring during interstadials. Therefore, despite the tuning of our model, the observed match between our result and that predicted by ss09sea is remarkable.

[38] At the moment, the “ss09sea” model provides the best available record of the annual layer thicknesses of the NorthGRIP core below 1800 m depth. However, as the absolute dating of the core advances our method can be tested against “true” annual layer thicknesses, and we believe that the VS profile has a strong potential for dating of the deeper part of the core (at least down to 2700 m

depth), where other profiles lack the resolution to resolve the annual layers.

6. Conclusions

[39] A high-resolution visual stratigraphy profile of the NorthGRIP ice core has been obtained for the depth interval 1330–3085 m. The record provides excellent core documentation and shows that the visual ice core stratigraphy is very regular down to a depth of 2600 m. Below this depth the stratigraphy gradually changes from a strictly horizontal pattern into a less well defined layering. In the deepest ice the ice crystal boundaries constitute the most prominent feature of the line scan images. The resolution of the VS record is higher than for any other profile measured on the

ice, and it enables identification of millimeter-sized features. The digital format of the profile enables clear visualization of very weak features by contrast adjustments.

[40] We found that it is important for the quality of the VS profile that the measurements are performed in the field shortly after recovery of the ice. The storing of the ice section down to 1750 m depth in the field has resulted in a significantly less well defined profile for that section. The same is true for the deepest part of the profile (below 2930 m depth), which was transported to Europe before being measured.

[41] Overall, the VS of the glacial ice shows a high degree of correlation with the impurity content of the ice. The best correlation occurs for the electrolytical conductivity, but there is also a very good correlation to the insoluble dust and Ca^{++} concentrations of the ice during periods with high dust concentrations. Because of this strong correlation, we interpret the cloudy bands in the glacial ice to be caused by these impurities, and we relate the intensity of the cloudy bands to the impurity content of the ice.

[42] A method for obtaining the annual layer thickness from the VS profile has been demonstrated. Briefly, the method consists of a frequency analysis of an idealized profile of the “most prominent” cloudy bands in the ice, which are identified from the VS profile. The method depends on a small number of parameters, which need to be calibrated. For this study, we have calibrated the method according to the timescale provided by the model “ss09sea.” The obtained annual layer thickness profile shows a strong correlation to climate with the thinnest annual layers occurring during the coldest periods, and a reduced thinning of annual layers toward the bottom of the ice in comparison to other Greenland locations with no bottom melt.

[43] Because our method is calibrated, we do not claim that our results provide an absolute dating of the NorthGRIP ice core. However, we do believe that the general pattern of increased annual layer thicknesses during interstadials is correctly recognized by the method, and we see VS as having a great potential for obtaining an ice core chronology for the deeper part of the NorthGRIP ice core at least down to 2700 m depth (90 kyr BP).

[44] **Acknowledgments.** This work is a contribution to the NorthGRIP ice core project, which is directed and organized by the Department of Geophysics at the Niels Bohr Institute for Astronomy, Physics and Geophysics, University of Copenhagen. It is being supported by funding agencies in Denmark (SNF), Belgium (FNRS-CFB), France (IFRTP and INSU/CNRS), Germany (AWI), Iceland (RannIs), Japan (MEXT), Sweden (SPRS), Switzerland (SNF) and the United States of America (NSF). This work is also a contribution to the Copenhagen Ice Core Dating Initiative that is supported by a grant from the Carlsberg Foundation.

References

Alley, R. B., A. J. Gow, D. A. Meese, J. J. Fitzpatrick, E. D. Waddington, and J. F. Bolzan (1997a), Grain-scale processes, folding, and stratigraphic disturbance in the GISP2 ice core, *J. Geophys. Res.*, *102*(C12), 26,819–26,830.

Alley, R. B., et al. (1997b), Visual-stratigraphic dating of the GISP2 ice core: Basic, reproducibility, and application, *J. Geophys. Res.*, *102*(C12), 26,367–26,381.

Barnes, P. R. F., R. Mulvaney, K. Robinson, and E. W. Wolff (2002), Observations of polar ice from the Holocene and the glacial period using the scanning electron microscope, *Ann. Glaciol.*, *35*, 559–566.

Barnes, P. R. F., E. W. Wolff, H. M. Mader, R. Udisti, E. Castellano, and R. Röthlisberger (2003), Evolution of chemical peak shapes in the Dome C, Antarctica, ice core, *J. Geophys. Res.*, *108*(D3), 4126, doi:10.1029/2002JD002538.

Bigler, M. (2004), Hochauflösende Spurenstoffmessungen an polaren Eisbohrkernen: Glazio-chemische und klimatische Prozessstudien, Ph.D. thesis, Univ. of Bern, Bern, Switzerland.

Dahl-Jensen, D., T. Thorsteinsson, R. Alley, and H. Shoji (1997), Flow properties of the ice from the Greenland Ice Core Project ice core: The reason for folds?, *J. Geophys. Res.*, *102*(C12), 26,831–26,840.

Dahl-Jensen, D., N. Gundestrup, H. Miller, O. Watanabe, S. J. Johnsen, J. P. Steffensen, H. B. Clausen, A. Svensson, and L. B. Larsen (2002), The NorthGRIP deep drilling program, *Ann. Glaciol.*, *35*, 1–4.

Gow, A. J., D. A. Meese, R. B. Alley, J. J. Fitzpatrick, S. Anandakrishnan, G. A. Woods, and B. C. Elder (1997), Physical and structural properties of the Greenland Ice Sheet Project 2 ice core: A review, *J. Geophys. Res.*, *102*(C12), 26,559–26,575.

Johnsen, S. J., D. Dahl-Jensen, N. Gundestrup, J. P. Steffensen, H. B. Clausen, H. Miller, V. Masson-Delmotte, A. E. Sveinbjörnsdóttir, and J. White (2001), Oxygen isotope and palaeotemperature records from six Greenland ice-core stations: Camp Century, Dye-3, GRIP, GISP2, Renland and NorthGRIP, *J. Quaternary Sci.*, *16*(4), 299–307.

Kipfstuhl, S., F. Pauer, W. F. Kuhs, and H. Shoji (2001), Air bubbles and clathrate hydrates in the transition zone of the NGRIP deep ice core, *Geophys. Res. Lett.*, *28*(4), 591–594.

Meese, D. A., A. J. Gow, R. B. Alley, G. A. Zielinski, P. M. Grootes, M. Ram, K. C. Taylor, P. A. Mayewski, and J. F. Bolzan (1997), The Greenland Ice Sheet Project 2 depth-age scale: Methods and results, *J. Geophys. Res.*, *102*(C12), 26,411–26,423.

North Greenland Ice-Core Project (NorthGRIP) Members (2004), High resolution climate record of the Northern Hemisphere reaching into the last Glacial Interglacial Period, *Nature*, *431*, 147–151.

Ram, M., and G. Koenig (1997), Continuous dust concentration profile of pre-Holocene ice from the Greenland Ice Sheet Project 2 ice core: Dust stadials, interstadials, and the Eemian, *J. Geophys. Res.*, *102*(C12), 26,641–26,648.

Ram, M., J. Donarummo Jr., M. R. Stolz, and G. Koenig (2000), Calibration of laser-light scattering measurements of dust concentration for Wisconsinan GISP2 ice using instrumental neutron activation analysis of aluminum: Results and discussion, *J. Geophys. Res.*, *105*(D20), 24,731–24,738.

Röthlisberger, R., M. Bigler, M. Hutterli, S. Sommer, B. Stauffer, H. G. Jungthans, and D. Wagenbach (2000), Technique for continuous high-resolution analysis of trace substances in firn and ice cores, *Environ. Sci. Technol.*, *34*(2), 338–342.

Ruth, U., D. Wagenbach, J. P. Steffensen, and M. Bigler (2003), Continuous record of microparticle concentration and size distribution in the central Greenland NGRIP ice core during the last glacial period, *J. Geophys. Res.*, *108*(D3), 4098, doi:10.1029/2002JD002376.

Shimohara, K., A. Miyamoto, K. Hyakutake, H. Shoji, M. Takata, and S. Kipfstuhl (2003), Cloudy band observations for annual layer counting on the GRIP and NGRIP, Greenland, deep ice core samples, *Mem. Natl. Inst. Polar Res., Spec. Issue*, *57*, 161–167.

Thorsteinsson, T., J. Kipfstuhl, and H. Miller (1997), Textures and fabrics in the GRIP ice core, *J. Geophys. Res.*, *102*(C12), 26,583–26,599.

Wang, Y., T. Thorsteinsson, J. Kipfstuhl, H. Miller, D. Dahl-Jensen, and H. Shoji (2002), A vertical girdle fabric in the NGRIP deep ice core, North Greenland, *Ann. Glaciol.*, *35*, 515–520.

M. Bigler and R. Röthlisberger, Climate and Environmental Physics, Physics Institute, University of Bern, Sidlerstrasse 5, CH-3012 Bern, Switzerland.

S. J. Johnsen, S. W. Nielsen, J. P. Steffensen, and A. Svensson, Department of Geophysics, University of Copenhagen, Juliane Maries Vej 30, DK-2100 Copenhagen Ø, Denmark. (as@gfy.ku.dk)

S. Kipfstuhl and U. Ruth, Department of Geophysics/Glaciology, Alfred Wegener Institute for Polar and Marine Research, P. O. Box 12 01 61, D-27515 Bremerhaven, Germany.